

Human Cartilage-Derived Progenitors Resist Terminal Differentiation and Require CXCR4 Activation to Successfully Bridge Meniscus Tissue Tears

CHATHURAKA T. JAYASURIYA , JOHN TWOMEY-KOZAK, JAKE NEWBERRY, SALOMI DESAI, PETER FELTMAN, JONATHAN R. FRANCO, NEILL LI, RICHARD TEREK, MICHAEL G. EHRlich,[†] BRETT D. OWENS

Key Words. Meniscus • Cartilage • Tissue repair • Stem cell • Progenitor • Chondroprogenitor • Hypertrophy

Department of Orthopaedics,
Brown University/Rhode
Island Hospital, Providence,
Rhode Island, USA

[†]Deceased.

Correspondence: Chathuraka T. Jayasuriya, Ph.D., B.A., Department of Orthopaedics, Brown University/Rhode Island Hospital, 1 Hoppin Street, Office 4.313, Providence, RI, 02903, USA. Telephone: (401)444-7837; e-mail: chathuraka_jayasuriya@brown.edu

Received July 16, 2018; accepted for publication September 5, 2018; first published online in *STEM CELLS EXPRESS* October 24, 2018.

<http://dx.doi.org/10.1002/stem.2923>

This is an open access article under the terms of the Creative Commons Attribution-NonCommercial License, which permits use, distribution and reproduction in any medium, provided the original work is properly cited and is not used for commercial purposes.

ABSTRACT

Meniscus injuries are among the most common orthopedic injuries. Tears in the inner one-third of the meniscus heal poorly and present a significant clinical challenge. In this study, we hypothesized that progenitor cells from healthy human articular cartilage (chondroprogenitor cells [C-PCs]) may be more suitable than bone-marrow mesenchymal stem cells (BM-MSCs) to mediate bridging and reintegration of fibrocartilage tissue tears in meniscus. C-PCs were isolated from healthy human articular cartilage based on their expression of mesenchymal stem/progenitor marker activated leukocyte cell adhesion molecule (ALCAM) (CD166). Our findings revealed that healthy human C-PCs are CD166+, CD90+, CD54+, CD106- cells with multilineage differentiation potential, and elevated basal expression of chondrogenesis marker SOX-9. We show that, similar to BM-MSCs, C-PCs are responsive to the chemokine stromal cell-derived factor-1 (SDF-1) and they can successfully migrate to the area of meniscal tissue damage promoting collagen bridging across inner meniscal tears. In contrast to BM-MSCs, C-PCs maintained reduced expression of cellular hypertrophy marker collagen X in monolayer culture and in an explant organ culture model of meniscus repair. Treatment of C-PCs with SDF-1/CXCR4 pathway inhibitor AMD3100 disrupted cell localization to area of injury and prevented meniscus tissue bridging thereby indicating that the SDF-1/CXCR4 axis is an important mediator of this repair process. This study suggests that C-PCs from healthy human cartilage may potentially be a useful tool for fibrocartilage tissue repair/regeneration because they resist cellular hypertrophy and mobilize in response to chemokine signaling. *STEM CELLS* 2019; 37:102–114

SIGNIFICANCE STATEMENT

The present study demonstrates that chondroprogenitor cell lines generated from healthy human articular cartilage can be used to facilitate successful bridging of inner meniscal tears in a manner that relies on SDF-1/CXCR4 chemokine axis. It is proof-of concept that C-PCs have the capacity to reintegrate and repair fibrocartilaginous tissue. Furthermore, this study reveals that C-PCs are resistant to terminal hypertrophic differentiation during the tissue repair process, unlike BM-MSCs.

INTRODUCTION

Meniscus injury is the second most common sports related knee injury [1]. Specifically, inner meniscal tears (white–white zone tears) present a significant clinical challenge because this area of tissue is avascular and consists of fibrocartilage that is sparse in cell number and capable of little to no healing [2]. Current clinical strategies for treating such injuries are limited to meniscectomy or resecting the area of damage in order to reshape it and remove

tattered tissue [3]. Unfortunately, both treatment options are reported to be significant risk factors of osteoarthritis (OA) development [4]. Prospective cell-based repair strategies have recently come to the forefront of meniscal injury research with the hopes of achieving better tissue repair in comparison to currently practiced clinical treatment strategies [5, 6].

Meniscus tissue injury repair using progenitor/stem cells is a topic of research that is being actively investigated. Many tissue specific mesenchymal stem cell (MSC) sources

(including bone marrow, fat, synovium, and meniscus itself) are being examined to identify the benefits associated with the usage of each in meniscus tissue repair [5, 7–10]. However, it can be argued that native progenitor cells residing in cartilaginous and fibrocartilaginous tissues are the likeliest of candidates to best fit this specialized role. For example, cells such as MSCs from bone marrow, synovium, and adipose tissue, which are also in consideration for fibrocartilage tissue repair do not have the advantage of coming from a similar biological microenvironment as the tissue which these cells are being used to repair. In this regard, articular cartilage-derived progenitor cells, which were first identified in 2004 [11], exist in a very similar biological milieu (i.e., cartilaginous microenvironment) that warrants their investigation in cell-based meniscal fibrocartilage repair. These cartilage progenitor cells (C-PCs) are reliably and easily distinguishable from mature articular chondrocytes based on their cell surface marker profile. Although cartilage-derived progenitors are a small population of cells [11], it may be feasible to isolate them for therapeutic use from non-weight-bearing areas of articular cartilage (i.e., linea terminalis and intercondylar notch) followed by *in vitro* expansion, akin to the strategy implemented during autologous chondrocyte implantation (ACI) [12].

In the present study, we generate clonal (pure and single cell derived) articular C-PC lines from young healthy human cartilage to characterize the heterogeneity of these progenitors. We use the most chondrogenic line to demonstrate for the first time that C-PCs can stimulate union of meniscus tissue tears. We report that C-PCs promote proliferation of native tissue meniscocytes and maintain significantly lower hypertrophy marker expression during meniscus tissue repair when compared with bone-marrow mesenchymal stem cells (BM-MSCs). This study provides first-time evidence that C-PCs can achieve bridging and integration of torn fibrocartilaginous tissue that make up the inner meniscus. Furthermore, it demonstrates that C-PCs will mobilize in response to stromal cell derived factor-1 (SDF-1), similar to BM-MSCs, and that inhibiting the SDF-1 receptor (CXCR4) in C-PCs adversely affects their ability to mediate tissue integration and repair in explant culture.

MATERIALS AND METHODS

Human Cartilage Progenitor Cell Isolation and Generation of Clonal Cell Lines

Human tissue was obtained with approval from the Rhode Island Hospital Institutional Review Board. Healthy knee articular cartilage was obtained from an 18-year-old female patient undergoing an amputation. Healthy cartilage was also obtained from viable graft tissue from a 24-year-old male. Cartilage tissue was brought to the laboratory within the hour, washed thoroughly in 1× Hanks' balanced saline solution (HBSS) and diced into very small pieces. The cartilage pieces were digested with Pronase (Roche, Indianapolis, IN; 2.0 mg/ml in 1× HBSS) for 30 minutes at 37°C in a shaking water bath. Cartilage pieces were washed in 1× HBSS and further digested using type IA Crude Bacterial Collagenase (Sigma-Aldrich, St. Louis, MO; 1.0 mg/ml) for 8 hours at 37°C in a shaking water bath. Cells were passed through a nylon cell strainer (100 µm pore size) to remove undigested tissue. Cells were washed three times in Dulbecco's modified Eagle's medium containing 10%

fetal bovine serum (FBS) (Dulbecco's modified Eagle's medium [DMEM]+). Enrichment of progenitor cells was achieved through fibronectin (FN) adhesion similar to previously described methods [13, 14]. A sterile 60 mm plastic petridish was immobilized with recombinant FN protein (10 µg/ml; PeproTech, Rocky Hill, NJ) in 0.1 M phosphate buffered solution (PBS) supplemented with 1.0 mM MgCl₂, 1.0 mM CaCl₂. Cells were seeded at low density onto the plate and placed in a 37°C cell incubator for 20 minutes. Cells that remained non-adherent to the plate in this time were washed away with 1× HBSS. Adherent cells were cultured in DMEM+. Single cells that formed a colony consisting of ≥32 cells within 10 days were individually isolated using cloning cylinders and replated separately. These individual colonies were grown for 1 week. Colonies were treated with pRetro-E2 SV40 (Applied Biological Materials Inc., Richmond, BC, Canada), according to the manufacturer. Four individual colonies (C-PC lines [CPCL]2, CPCL3, CPCL4, CPCLA1) were successfully immortalized becoming clonal C-PC lines. Cell lines and primary C-PCs were cultured and maintained in DMEM with 10% FBS, 1% Pen Strep, 100 mM HEPES, 2 mM L-glutamine, 0.1 mM ascorbic acid, 0.1 mM sodium pyruvate, and 2.7 µM L-glucose (DMEM++).

Explant Meniscus Repair Culture Conditions

Three-month-old Lewis rats were euthanized in accordance with approvals from the Institutional Animal Care and Use Committee of Rhode Island Hospital. Menisci were isolated using sterile tools, rinsed with sterile PBS, and cultured in DMEM++ in a 37°C cell incubator for 24–48 hours prior to experiments. For explant repair experiments, at least three menisci were used per experimental group. A radial tear was created in the inner anterior horn and each meniscus was placed into a 96-well culture plate. Torn menisci were treated by coculturing with 1.0×10^5 healthy human primary BM-MSCs (ATCC, Manassas, VA), CPCL3, primary C-PCs, or no cell (control group). All cells were fluorescently labeled with Vibrant Dil Cell Labeling Solution (ThermoFisher Scientific, Waltham, MA) according to the manufacturer. In experiments involving SDF-1, menisci were pre-treated with SDF-1 recombinant protein (200 ng/ml; PeproTech Inc.) for 15 minutes followed by treatment with 1.0×10^5 fluorescently labeled CPCL3 cells. Images were taken 3, 5, 10, 17, and 20 days after treatment using a Nikon Eclipse TS2 microscope. Gene expression analysis was conducted using mRNA collected from 20 day samples.

C-PC/BM-MSC Conditioned Media Experiments

To obtain conditioned medium, C-PCs and BM-MSCs were seeded (1.0×10^5 cells/well) into 6-well plates and cultured in DMEM++ (2 ml per well). Cells were cultured for 4 days in a 37°C cell incubator. Medium was collected, centrifuged (1,700 rpm, for 5 minutes) and supernatant was used as conditioned media. Meniscocytes were isolated from rat menisci from 3-month-old Lewis rats. Menisci were diced into small fragments, digested with Pronase (Roche; 2.0 mg/ml in 1× HBSS) for 30 minutes at 37°C in a shaking water bath, washed in 1× HBSS and further digested using type IA Crude Bacterial Collagenase (Sigma-Aldrich; 1.0 mg/ml) for 8 hours at 37°C in a shaking water bath. Cells were passed through a nylon cell strainer (100 µm pore size) to remove undigested tissue. Meniscocytes were expanded in DMEM++ in a 37°C cell incubator prior to experiments. Meniscocytes were seeded

(5.0×10^4 cells/well) into a 12-well plate. After 24 hours, media was changed to 600 μ l of conditioned media from BM-MSC, CPCLA1, CPCL3, or unconditioned *DMEM*++ media (control). Cells were cultured for 6 days and cell numbers were quantified using a hemocytometer. Images were taken using a Nikon Eclipse TS2 microscope.

Tissue Immunohistochemistry and Staining

Human articular cartilage tissues and rat meniscal tissues were fixed in formalin solution for 72 hours, and placed in 70% ethanol solution for 24 hours. Rat meniscal tissues were also decalcified in 10% EDTA solution for 24 hours. Tissue was embedded in paraffin and sections (4.0 μ m thick) were mounted onto glass slides, cleared using xylene, and gradually rehydrated. Antigen retrieval was performed on slides using sodium citrate buffer (10 mM sodium citrate and pH 6) at 100°C for 20 minutes. Slides were cooled and rinsed in distilled water to remove citrate solution. Slides were blocked using Super Block (ThermoFisher Scientific) for 1 hour at room temperature. Slides were stained with a monoclonal mouse antibody (1:100 in TBS, 1% BSA) against human CD166 (Abcam, Cambridge, MA), overnight at 4°C. Sections were washed three times in Tris Buffered Saline with Tween-20 (TBST) and incubated with anti-mouse secondary antibody Alexa Fluor ab150105 (Abcam) diluted 1:1,000 for 30 minutes at room temperature. Sections were washed three more times in TBST. Mounting solution containing Dapi was added and sections were coverslipped. For slides stained with Masson's Trichrome, sections were stained with Trichrome Stain LG solution (Sigma-Aldrich) and Weigert's Iron Hematoxylin (Sigma-Aldrich) according to the manufacturer. Picro Sirius Red Stain Kit (Connective Tissue Stain; Abcam) was also used to stain sections according to the manufacturer. For slides stained with hematoxylin and eosin (H&E), sections were cleared and rehydrated followed by staining with H&E, according to standard protocols. Sections were then dehydrated gradually and mounted for imaging. All images were acquired using a Nikon Eclipse 90i Digital Imaging System.

Messenger RNA Expression Analysis

Real-time quantitative polymerase chain reaction (RT-qPCR) was used to quantify mRNA expression levels. Forward and reverse primer sequences corresponding to each tested gene are listed in Table 1. Total mRNA was isolated from tissue and/or cells via RNAqueous Kit (Ambion, Austin, TX) according to manufacturer. Messenger RNA was reverse transcribed into cDNA using iScript cDNA Synthesis Kit (Bio-Rad, Hercules, CA) according to the manufacturer. Messenger RNA levels were calculated using the delta delta Ct ($\Delta\Delta$ Ct) method and normalized to one of two house-keeping genes (ribosomal RNA 18S or beta-actin). $X = 2^{-\Delta\Delta$ Ct}, in which $\Delta\Delta$ Ct = (Ct_{Exp target gene} -

Ct_{Exp house-keeping gene}) - (Ct_{Ctl target gene} - Ct_{Ctl house-keeping gene}) and X = relative transcript; Ct_{Exp} = Ct of experimental group, Ct_{Ctl} = Ct of control group.

Cell Surface Marker Analysis

Cell surface markers were analyzed by flow cytometry. Antibodies pre-conjugated with dye were used. CD54(PE), CD90 (FITC), CD106(APC), CD166(APC), and IgG isotype control antibodies were purchased from Miltenyi Biotec Inc., San Diego, CA. Cells (1.0×10^6) were detached, washed in 5 ml of 1 \times PBS, spun down in a centrifuge at 300g and resuspended in 100 μ l of buffer (1 \times PBS, 0.5% bovine serum albumin, and 2 mM EDTA). Pre-conjugated antibody (10 μ l) was added, mixed gently, and incubated with the cells in the dark at 4°C for 10 minutes. Excess antibody was washed off with 1.0 ml of 1 \times PBS. Stained cells were resuspended in 500 μ l of buffer and analyzed using Accuri C6 Flow Cytometer (BD Biosciences, San Jose, CA).

Stem Cell Differentiation Analysis

The chondrogenic, adipogenic, and osteogenic differentiation capacities of clonal cartilage-derived stem cell lines were analyzed in vitro. Cells were seeded at a density of 1.0×10^4 cells/well in 12-well plates. Each well received 1.0 ml of cell suspension at the beginning of each differentiation assay. For chondrogenesis assay, cells were cultured in serum free chondrogenesis medium or *DMEM*++ (growth medium control group), for 10 days and 21 days. Chondrogenesis medium consisted of high-glucose *DMEM* supplemented with 40 mg/ml L-proline, 100 nM dexamethasone, 50 mg/ml ascorbic acid, 1% Gibco Insulin Transferrin Selenium premix (ThermoFisher Scientific), 10 ng/ml TGF- β 3 (PeproTech Inc.) [15]. Medium was freshly changed every 72 hours. At the time of analysis, wells were washed with 1 \times PBS and fixed with ice cold methanol for 10 minutes at -20°C. Methanol was removed and cell monolayers were gently washed with distilled water. Alcian blue (0.2% solution, in 0.1 M HCl, pH 1.0) was added (0.5 ml) to each well and incubated overnight at room temperature. After incubation, Alcian blue solution was removed and the cell monolayers were gently washed once with 0.1 M HCl and three times in distilled water. Stained cell monolayers were imaged using a Leica MZ6 dissecting microscope. Staining intensities were quantified by extracting the color from stained monolayers by incubating with 300 μ l of 6 M GuHCl overnight at room temperature under gentle shaking conditions. One hundred microliters of extracted color solution from each well was used to quantify staining via microplate reader. For adipogenesis assay, cells were cultured in Stempro Adipogenesis differentiation media (Life Technologies, Grand Island, NY) or *DMEM*++ (growth medium control group), for 21 days. Medium was freshly changed every 72 hours. At the time of analysis, wells were washed with

Table 1. List of forward and reverse primers, in 5' to 3' orientation, used for real-time quantitative PCR

Gene	Forward seq.	Reverse seq.	Accession
ITGA5	GGCTTCAACTTAGACGCGGA	ATTCATGGGGGTGCACTGT	NM_002205.4
SOX9	GGACCACTACCCGCACTTGCA	GTTCTTCACCGACTTCTCCGCCG	NM_000346.3
ACAN	ACCAGACGGGCTCCAGAC	ACAGCAGCCACACCAGGAAC	NM_001135.3
COL1A1	CAGGAGGCACGCGGAGTGTG	GGCAGGGCTCGGGTTCCAC	NM_000088.3
COL2A1	CTCCCAGAACATCACCTACCACT	CGTGAACCTGTATTGCCCT	NM_001844.4
COL10A1	GCCACAGGCATAAAAAGGCC	GAAGGACCTGGGTGCCCTCGA	NM_000493.3
LPL	GACACTTGCCACCTCATTC	AGCCATGGATCACCATGAAGG	NM_000237.2
ALPL	CTGGACGGACCTCGCCAGTG	TGCAATCGACGTGGGTGGGAGG	NM_000478.5
Beta-Actin	GGACCTGACTGACTACCTCAT	CGTAGCACAGTCTCTCTTAAT	NM_001101.4

1× PBS. Cell monolayers were fixed using 10% formalin for 5 minutes at room temperature. Monolayers were stained with 0.3% Oil Red-O solution in isopropanol for 10 minutes, stain was removed and monolayers were gently washed four times with distilled water. Images were acquired using a Nikon Eclipse TE2000 inverted microscope. For osteogenesis assay, cells were cultured in Stempro Osteogenesis differentiation media (Life Technologies), for 21 days. Medium was freshly changed every 72 hours. At the time of analysis, wells were washed with 1× PBS. Cell monolayers were fixed using 10% neutral buffered formalin for 30 minutes at room temperature. Monolayers were stained with 2% alizarin red solution (pH 4.1) for 30 minutes. Staining solution was carefully aspirated and the monolayers were gently washed four times with distilled water. Images were acquired using Nikon Eclipse TE2000 inverted microscope.

Western Blot Analysis

Total protein was extracted from BM-MSCs and CPCL3 cell line (50,000 cells/well) using 1× RIPA buffer containing 1 mM PMSF (Cell Signaling Technology, Danvers, MA). BM-MSCs and nCPCL3 were washed with sterile cold PBS. The lysis extract was collected and centrifuged at 12,000 rpm for 10 minutes at 4°C. The concentration of total protein supernatant was determined using Pierce BCA Protein Assay kit (ThermoFisher Scientific), according to the manufacturer. Then, 3× blue loading buffer containing DTT, reducing agent (Cell Signaling Technology) was added in equal proportion and mixed in the protein. The sample was boiled for 10 minutes at 95°C. Equal amounts of protein were resolved on 4%–15% Mini-PROTEAN TGX Precast Gels (Bio-Rad). Blots were transferred to PVDF membrane (Bio-Rad) overnight at a constant voltage of 22 V. The membrane was blocked for 1 hour at room temperature with 5% Nonfat Dry Milk (Cell Signaling Technology) in TBST (0.1%). The membrane was incubated at 4°C overnight with specific primary antibodies, Col X (Abcam) and β -Actin (Cell Signaling Technology) at 1:500 dilution and 1:1,000 dilution, respectively. Secondary antibodies IRDye 800CW Goat anti-rabbit (diluted 1:5,000) and IRDye 680RD Goat anti-mouse (diluted 1:5,000; LI-COR Biosciences, Lincoln, NE) were used by incubating with membrane for 2 hours at room temperature. Membranes were imaged using an Odyssey fluorescence scanner (LI-COR Biosciences).

Statistics

Statistical analysis using a Student's *t* test was performed on experiments containing two groups, or experiments that compared each experimental group to a single control group. One-way analysis of variance (ANOVA) and post hoc analysis (Dunnett's Multiple Comparison test or Tukey test) was used when analyzing data from experiments with more than two experimental groups that required comparisons between every group. $N \geq 3$ for all experiments. Error bars illustrate ± 1 standard deviation of the mean. A *p*-values smaller or equal to .05 was considered statistically significant.

RESULTS

Stable Human C-PC Lines Retain Chondroprogenitor Cell Properties

Healthy articular cartilage contains a sparse population of C-PCs [11, 13]. We sought to generate clonal human C-PC lines that can be used for molecular characterization and (potentially) tissue

repair. Mesenchymal stem/progenitor cell marker activated leukocyte cell adhesion molecule (ALCAM) (CD166) has previously been used to distinguish progenitor cell populations from mature chondrocytes in healthy adult articular cartilage [16]. Staining for CD166 with a fluorescent antibody allows visualization of C-PCs in healthy human femoral condyle cartilage tissue (Fig. 1A). Human articular cartilage was digested to release resident cells and these cells were sorted using an antibody against CD166, similar to previously described methods [14]. Primary C-PCs (CD166+ cells) were compared with primary mature chondrocytes (CD166- cells) by means of mRNA expression analysis. C-PCs exhibited elevated basal mRNA expression levels of FN receptor (ITGA5) in comparison to chondrocytes (Fig. 1B). Chondrocyte transcription factor SOX9 and cartilage proteoglycan protein aggrecan (ACAN) mRNA levels were decreased in C-PCs, relative to chondrocytes (Fig. 1B), whereas fibrochondrocyte marker type I collagen (COL1A1) mRNA expression levels were increased in C-PCs. Primary C-PCs expressed MSC surface markers CD90, CD166, and the chondrocyte marker CD54 (Fig. 1C). Primary C-PCs did not express vascular cell adhesion protein VCAM1 (CD106), confirming that they are not endothelial cells.

Considering their elevated ITGA5 expression, primary heterogeneous C-PCs were enriched through differential adhesion to FN as previously described [11]. Individual C-PCs isolated in this manner were clonally expanded and stabilized using retroviral Large T antigen to generate single cell-derived lines. Four different single cell derived C-PC lines (CPCL) were successfully generated (Fig. 2). Relative mRNA expression of FN receptor ITGA5, chondrogenesis transcription factor SOX9, fibrochondrocyte marker collagen I (COL1A1), and chondrocyte hypertrophy marker collagen X (COL10A1) were quantified across the C-PC lines by RT-PCR. Primary BM-MSCs and primary chondrocytes were used as controls. CPCL2, CPCL3, and CPCL4 exhibited the highest expressional fold change (eightfold, ninefold, and eightfold, respectively) of ITGA5 relative to chondrocytes (Fig. 3A). SOX-9 mRNA expression level was highest in chondrocytes with CPCL3 coming in second highest, suggesting that it is the line that is most committed to the chondrocyte lineage (Fig. 3B). Indeed, CPCL3 exhibited nearly twofold higher expression of SOX9, compared with the BM-MSC group. Fibrochondrocyte marker COL1A1 expression was highest in BM-MSCs (Fig. 3C). However, all C-PC lines exhibited higher COL1A1 levels than the chondrocyte group (Fig. 3C). Finally, hypertrophy marker COL10A1 was lowest in CPCL2, CPCL3, and CPCL4 (<0.25-fold, relative to the chondrocyte group; Fig. 3D). COL10A1 expression was highest in the BM-MSC group (>20-fold, relative to the chondrocyte group). Although these results demonstrate heterogeneity across the generated lines, all lines strictly exhibited higher expression levels of fibrochondrocyte marker COL1A1 than mature chondrocytes. All cell lines also exhibited lower expression of hypertrophy marker COL10A1 than mature chondrocytes and BM-MSCs. These two features were primary motivations for us to test the repair capacity of C-PCs in meniscus tissue, which has high collagen I content.

Cell Surface Marker Profile and Differentiation Capacity of Human C-PC Lines

We verified that the generated stable human C-PC lines exhibited a cell surface marker profile that is consistent with that of primary C-PCs. This was done to ensure that stabilization of the clonal C-PCs using Large T-Antigen did not dramatically alter their cellular phenotype. Two of the generated cell lines (CPCLA1 and CPCL3)

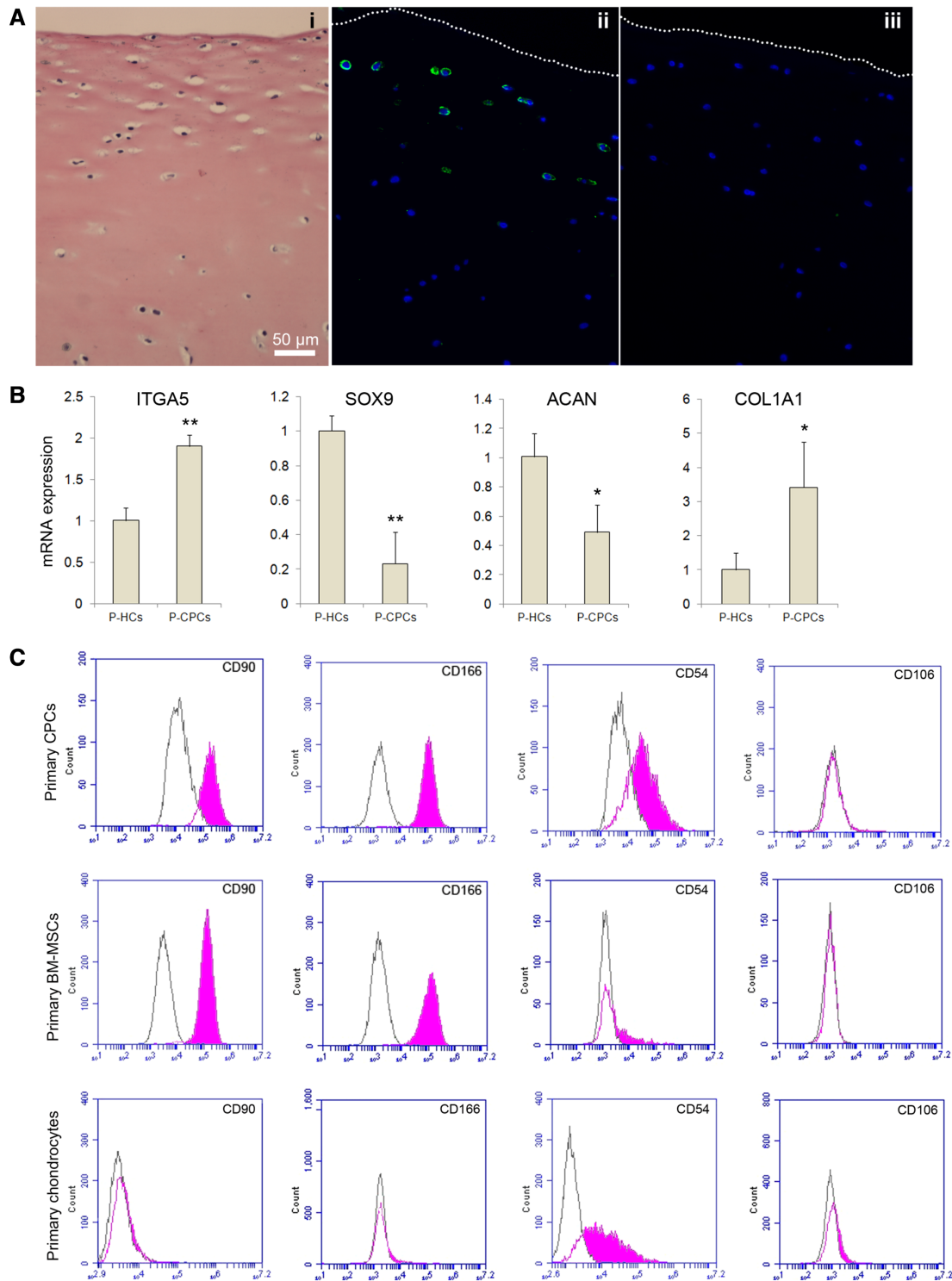


Figure 1. Visualization and molecular characterization of primary chondroprogenitor cells from healthy human articular cartilage. **(A):** Hematoxylin and eosin staining of human knee articular cartilage from 18-year-old amputee (i). Immunofluorescent staining of cartilage section for mesenchymal stem cell marker ALCAM/CD166 (green) and Dapi nuclear stain (blue) (ii). IgG control antibody staining (iii) demonstrates the absence of nonspecific immunofluorescent staining. **(B):** Relative mRNA expression levels of fibronectin receptor (ITGA5), chondrocyte markers (SOX9, ACAN), and fibrochondrocyte marker (COL1A1) in primary cartilage chondroprogenitors (P-CPCs) and primary chondrocytes (P-HCs). $N \geq 3$; *, $p \leq .05$; **, $p \leq .01$ relative to P-HC group. Quantitative data are represented as mean \pm SD. **(C):** Cell surface marker profiles of P-CPCs, bone-marrow derived mesenchymal stem cells (BM-MSCs), and P-HCs as determined using flow cytometry. Filled peaks indicate the percentage of cells that stained positively for each antibody. Empty peaks represent the results of cells stained with isotype control antibodies.

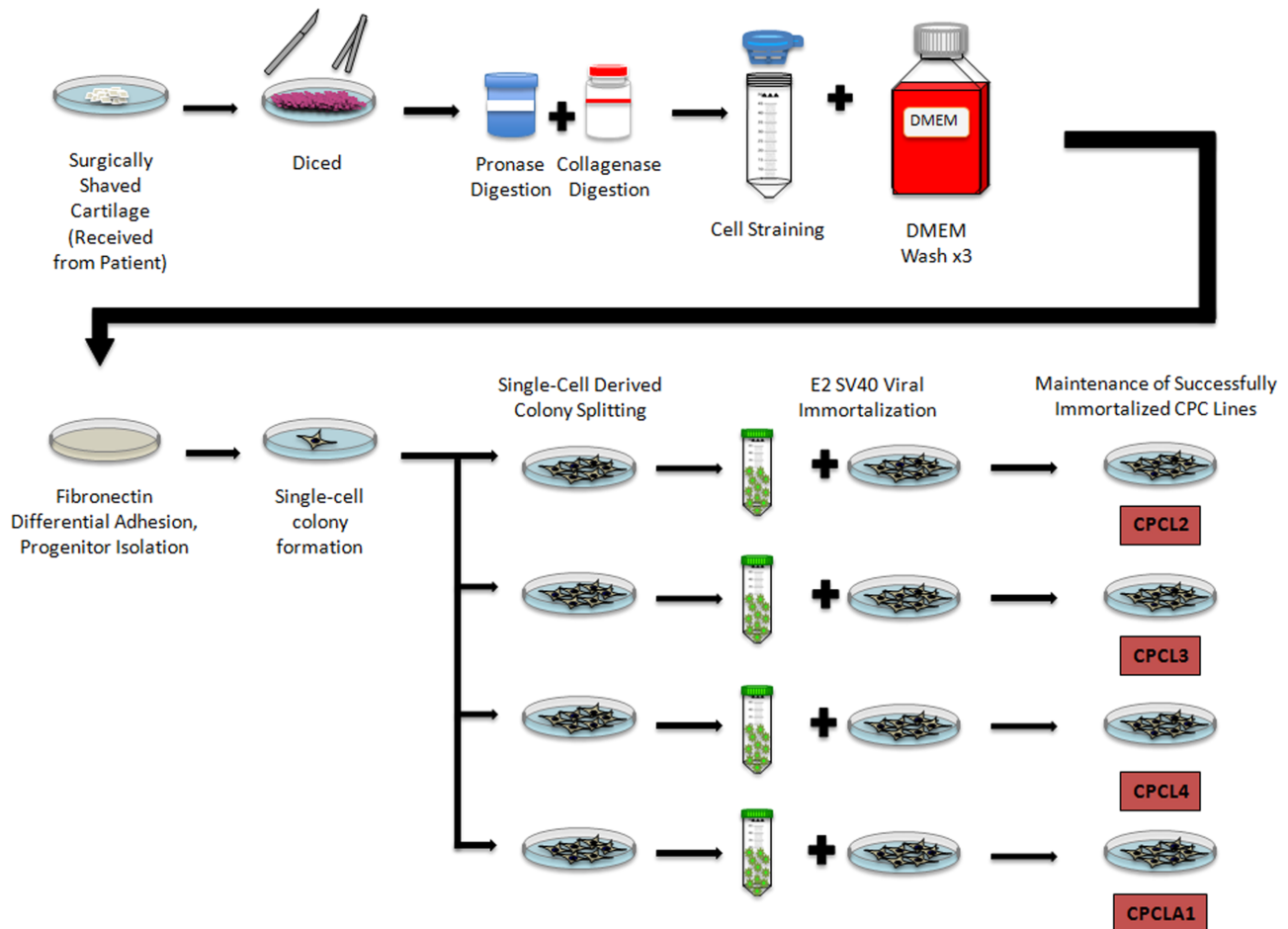


Figure 2. Establishment of healthy human articular cartilage-derived progenitor cell lines. Illustrated diagram of procedure used to establish human cartilage progenitor cell lines. Healthy human cartilage was diced into small pieces and digested using pronase and collagenase. Released cells were washed and strained to remove clumps. Cells were seeded at low density and individual single-cell derived colonies were separated and stabilized using SV-40 mediated delivery of large-T antigen.

were used to conduct this validation. We specifically selected these two clones because of their different expression of chondrogenesis regulator SOX9. We confirmed that CPCLA1 and CPCL3 were both largely positive for CD90 (Fig. 3E), similar to primary C-PCs (Fig. 1C). However, CPCL3 contained noticeably fewer CD90+ cells (~55%) than did CPCLA1 (~80%). CPCLA1 and CPCL3 both stained positively for CD166 and negatively for endothelial marker CD106 (Fig. 3E). Overall, these findings suggest that generated C-PC lines exhibit a cell surface marker profile that is largely consistent with that of primary C-PCs shown in Figure 1C.

CPCLA1 and CPCL3 were used to characterize the differentiation capacities of stable C-PC lines. CPCLA1 and CPCL3 were both capable of chondrogenic differentiation as demonstrated by positive Alcian blue staining for proteoglycan deposition following culturing in chondrogenesis medium (Fig. 4A, 4B). In both cell lines, Alcian blue staining intensities increased from day 10 to day 21 of culture in chondrogenesis medium. At day 21, CPCL3 exhibited the formation of deeply blue stained chondrogenic nodules, as indicated by black arrowheads (Fig. 4A, bottom right panel), which was indicative of enhanced proteoglycan accumulation. Alcian blue staining intensities were elevated sixfold in CPCL3, following 21 days of culturing in chondrogenesis medium in comparison to the threefold (only) increase that was observed in CPCLA1 (Fig. 4B). Relative

mRNA expression of chondrocyte marker COL2A1 was observed to be significantly elevated by six- to eightfold in both cell lines during chondrogenesis induction (Fig. 4C).

Both cell lines were demonstrated to be capable of adipogenic differentiation; however, this capacity seemed significantly higher in CPCLA1 (Fig. 4D, left panels, 4E). Oil Red O staining for lipid accumulation demonstrated that CPCLA1 and CPCL3 produced lipid droplets following 21 days of culture in adipogenesis medium (Fig. 4D, left panels). Quantification of lipopolyphase (LPL) mRNA revealed that CPCLA1 exhibited significantly greater expression of LPL (60-fold increase) following 5 days of culture in adipogenesis medium, whereas CPCL3 only exhibited a 3.5-fold elevation of LPL under the same conditions (Fig. 4E).

Both cell lines were also demonstrated to be capable of osteogenic differentiation as indicated by staining and mRNA quantification of alkaline phosphatase (Fig. 4D, right panels, 4F). However, CPCL3 exhibited lower osteogenesis potential compared with CPCLA1, based on staining analysis. Alizarin red staining for mineralization following 21 days of culture in osteogenesis medium demonstrates that staining intensities were greatly reduced in CPCL3, indicating that this line has a low propensity for ossification in comparison to CPCLA1 (Fig. 4D, right panels).

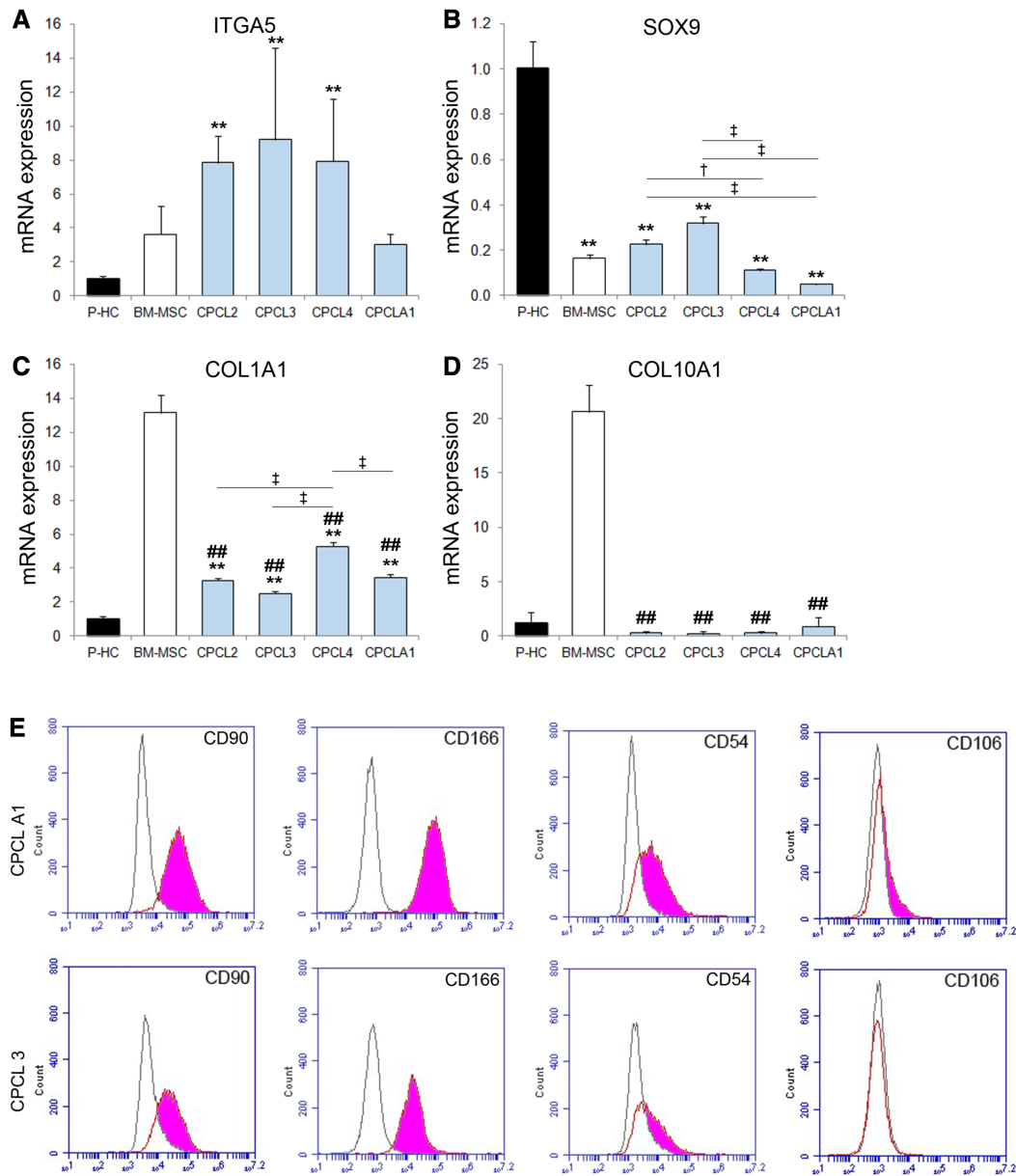


Figure 3. Molecular characterization of generated clonal chondroprogenitor cell lines from healthy human cartilage. **(A):** Relative mRNA expression of ITGA5; **(B):** SOX9; **(C):** COL1A1; and **(D):** terminal differentiation and hypertrophic marker COL10A1 in primary human chondrocytes, bone-marrow derived mesenchymal stem cells (BM-MSCs), and four clonal cartilage chondroprogenitor cell lines. $N \geq 3$; *, $p \leq .05$; **, $p \leq .01$ relative to P-HC group; †, $p \leq .05$; ‡, $p \leq .01$ between indicated groups. A Dunnett's test was used for post hoc analysis of ITGA5 mRNA quantities; a Tukey test was used for analysis of SOX9, COL1A1, and COL10A1 mRNA quantities. Quantitative data are represented as mean \pm SD. **(E):** Cell surface marker profiles of two stable clonal CPC cell lines (CPCLA1 and CPCL3) as determined using flow cytometry. Filled peaks indicate the percentage of cells that stained positively for each tested antibody. Empty peaks represent the results of cells stained with isotype control antibodies.

Chondroprogenitors from Human Articular Cartilage Promote Meniscal Fibrochondrocyte Proliferation and Tissue Integration

To examine the reparative capabilities of articular cartilage derived chondroprogenitor cells, we created a radial tear in the white-white (ww) zone of rat menisci and treated them with fluorescently labeled CPCL3 (1.0×10^5) in an explant culture system (Fig. 5A, 5B). CPCL3 was specifically selected for this treatment for several reasons. CPCL3 has reduced osteogenic potential (Fig. 4D) and high expression of chondrogenesis marker SOX9 (Fig. 3B), in comparison to CPCLA1. Furthermore,

treatment of murine (rat) meniscal fibrochondrocytes with conditioned media from CPCL3 induced greater than 100% increase in fibrochondrocyte proliferation, whereas BM-MSCs and CPCLA1 each induced 60% increase (Supporting Information Fig. S1). As such, it was hypothesized that CPCL3 exhibited the most suitable biological repertoire and stimulated paracrine effects on the local meniscus fibrochondrocyte cell population to be most conducive to meniscal tissue repair/regeneration.

CPCL3 treatment resulted in reintegration of the torn tissue within 25 days, whereas this was not observed in the untreated control group (Fig. 5A). Subsequent histological

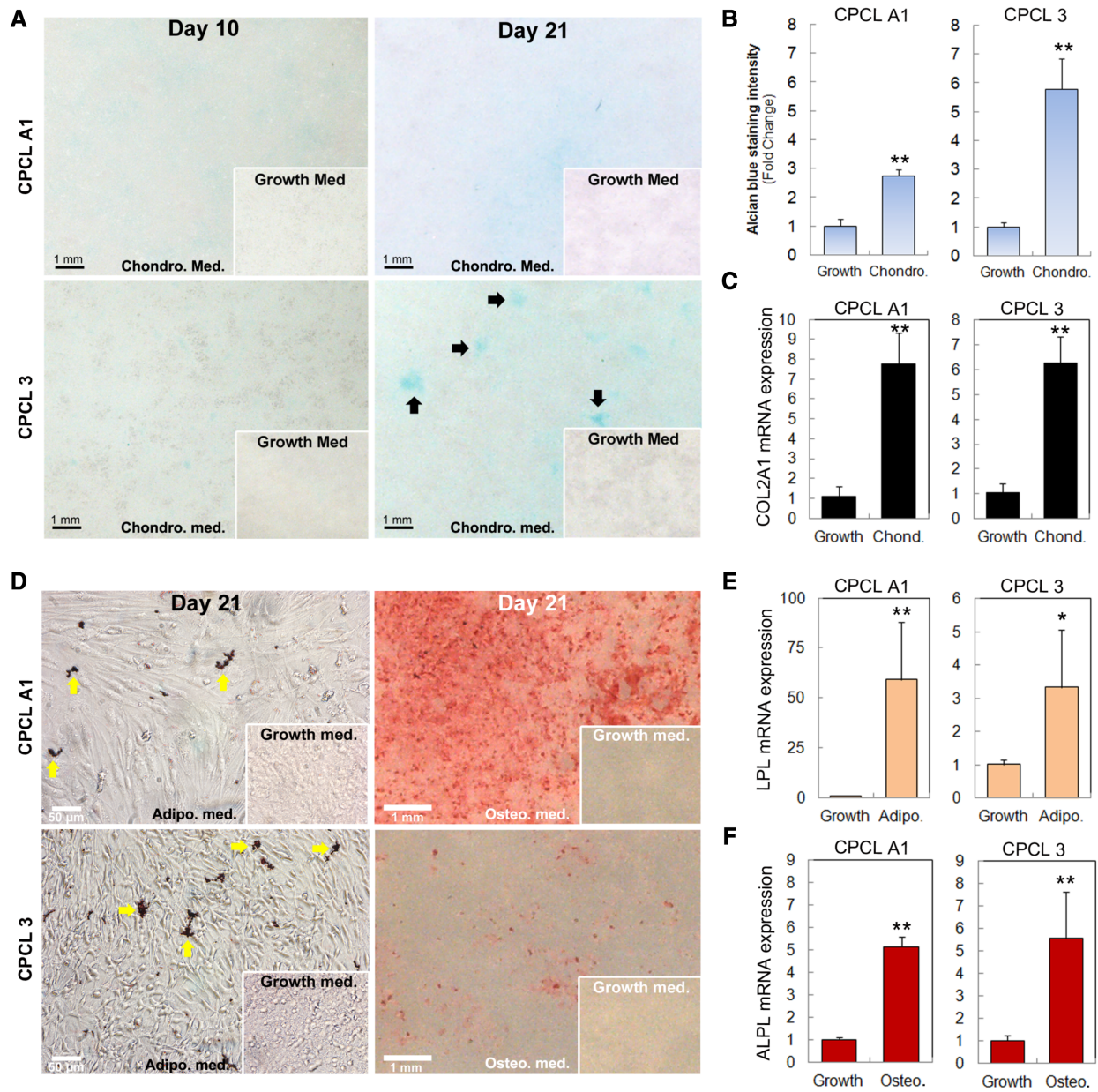


Figure 4. Cartilage chondroprogenitor cell line (CPCL)3 exhibits high chondrogenic potential and low adipogenic and osteogenic potential. **(A):** Alcian blue staining of CPCLA1 and CPCL3 following 10 days and 21 days of culturing in chondrogenesis medium or growth medium. Black arrows indicate chondrogenic nodules that formed only in CPCL3 following 21 days in chondrogenesis medium. **(B):** Fold change of Alcian blue staining intensities following 21 days of culturing CPCLA1 and CPCL3 in chondrogenesis medium or growth medium. **(C):** Collagen 2 (COL2A1) mRNA expression levels in CPCLA1 and CPCL3 following 5 days of culturing in chondrogenesis medium or growth medium. **(D):** Oil red O staining for lipid droplet formation following 21 days of culturing CPCLA1 and CPCL3 in adipogenesis medium or growth medium (left panels). Yellow arrows indicate lipid droplet accumulation. Alizarin red staining for mineralization following 21 days of culturing CPCLA1 and CPCL3 in osteogenesis medium or growth medium (right panels). **(E):** Lipopolyllipase (LPL) mRNA expression levels in CPCLA1 and CPCL3 following 5 days of culturing in adipogenesis medium or growth medium. **(F):** Alkaline phosphatase (ALPL) mRNA expression levels in CPCLA1 and CPCL3 following 5 days of culturing in osteogenesis medium or growth medium. $N \geq 3$; *, $p \leq .05$; **, $p \leq .01$ relative to respective control groups that were cultured in growth medium.

analysis revealed that CPCL3 treatment resulted in matrix bridging and tissue integration along the tear channel as indicated by Masson’s Trichrome staining and Picro Sirius Red staining for collagen networks, respectively (Fig. 5B, 5D). Control menisci that were not treated with cells exhibited no signs of tissue integration as these tear channels remained opened.

Time lapse images taken at 3 days, 10 days, and 20 days after treatment show fluorescently labeled CPCL3 progressively

filling a longitudinal meniscal tear by day 20 in explant culture (Fig. 5C). Control menisci treated with fluorescently labeled BM-MSCs were incapable of completely filling the defect within the same time period. It was confirmed that treatment with primary C-PCs (not cell line) would also achieve defect filling within 20 days (Fig. 5G). Quantification and analysis of human mRNA transcripts indicated that human COL1A1 expression in CPCL3 and primary BM-MSCs did not significantly

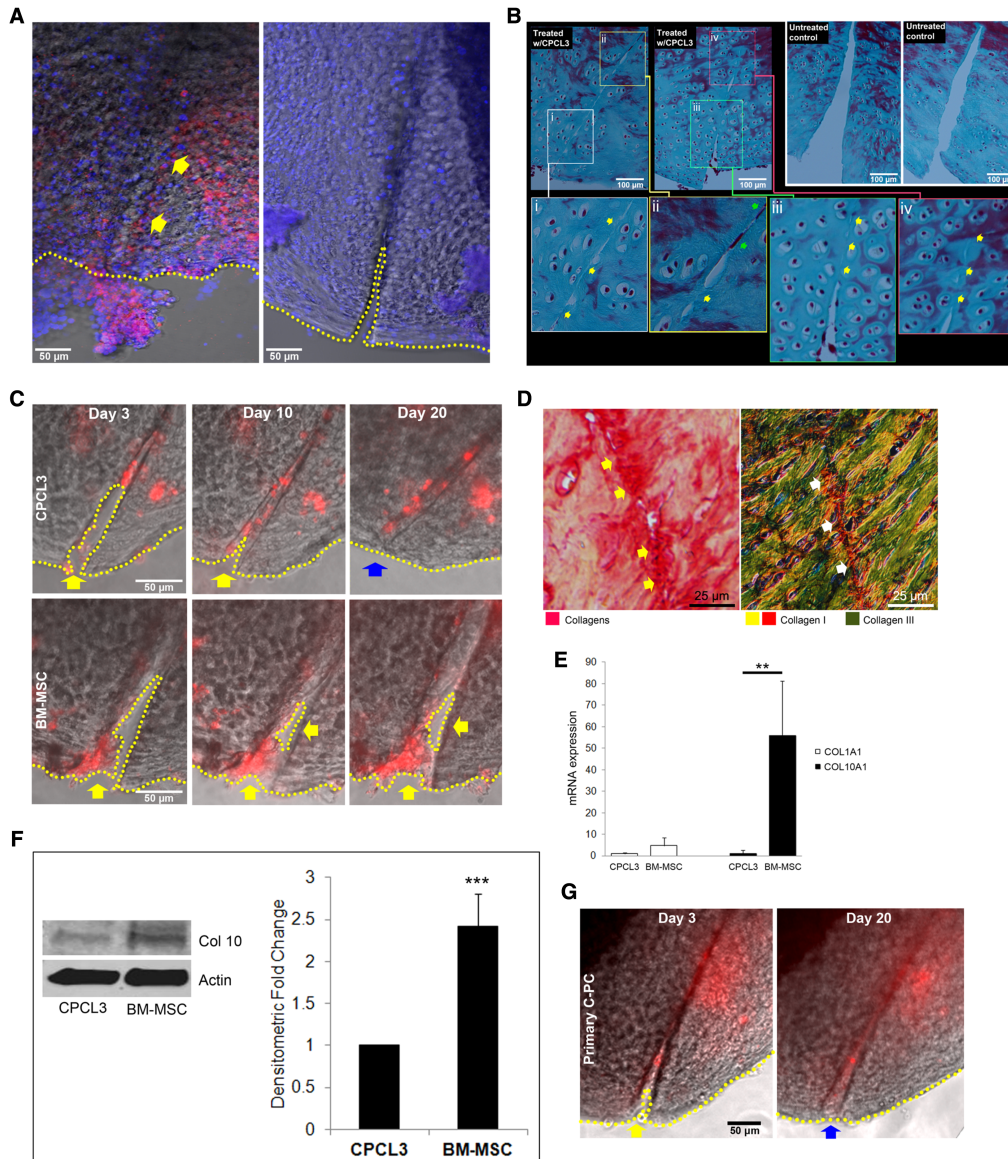


Figure 5. Cartilage chondroprogenitors stimulate filling and integration of torn rat menisci. **(A):** Whole tissue mount confocal images of radial tears in rat menisci that were either treated with fluorescently labeled chondroprogenitor cell line (CPCL3) (1.0×10^5 cells; left) or untreated (right) for 4 weeks, in explant culture. Nuclear staining was achieved using Dapi (blue). Arrows signify filled cut channel. Dotted lines help signify union (left) and nonunion (right) of the tissue periphery. **(B):** Trichrome stained 4 μ m thick histological sections of radial tears in rat menisci that were either treated with CPCL3 (1.0×10^5 cells) or left untreated (collagens stain blue; cell nucleus and cytoplasm stain purple/red). Samples were fixed, embedded in paraffin, and sectioned 4 weeks following treatment. Green arrows indicate cells that have adhered and bridge the tear channel. Yellow arrows indicate integrating regions of the tear channel. **(C):** Time lapse images of inner anterior horn tears in rat menisci treated with 1.0×10^5 fluorescently labeled CPCL3 or BM-MSCs. Images were taken at day 3, day 10, and day 20 following treatment. Images are representative of results observed for each respective group. Experiments were repeated more than three times. **(D):** Histology analysis of CPCL3 mediated integration of a rat meniscal tear stained with Picrosirius red and imaged under normal light (left panel) and polarized light (right panel) shows different collagen species and their distribution along the cut channel. Red staining indicates collagen fibrils and arrows indicate points of collagen bridging across the tear channel (left panel). Type I collagen bridging is indicated with arrows across the tear channel (right panel). **(E):** Human specific type I collagen and type X collagen mRNA expression was quantified and compared between CPCL3 and BM-MSCs, after tissue integration. $N \geq 3$; **, $p \leq .01$ compared with BM-MSC control group. **(F):** Basal type X collagen produced by CPCL3 and BM-MSCs as analyzed by Western blot following 7 days in culture. Beta-actin was used as a loading control. Blots were independently performed three times. ImageJ was used to make densitometric quantification of type X collagen bands between CPCL3 and BM-MSC groups, normalized to their respective beta-actin bands that were used as loading controls. $N = 5$; ***, $p \leq .005$. **(G):** Images of inner anterior horn tears in rat menisci treated with 1.0×10^5 fluorescently labeled primary C-PCs. Images were taken at day 3 and day 20 following treatment. Dotted lines indicate tissue periphery and gaps in filling. Yellow arrow indicates gaps in filling of the tear channel. Blue arrow indicates complete filling of the tear channel. Experiments were repeated three times.

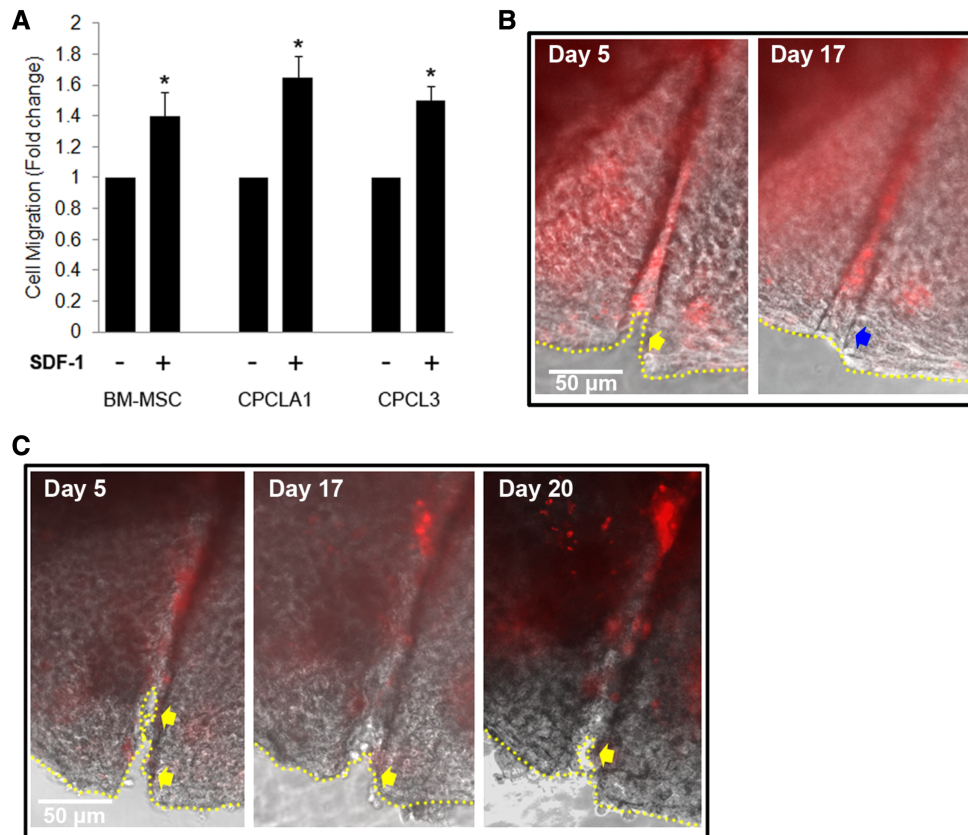


Figure 6. Inhibition of SDF-1/CXCR4 axis impairs cartilage chondroprogenitor cell mediated filling of meniscal tears. **(A):** Transwell assay results of bone-marrow derived mesenchymal stem cells (BM-MSCs), chondroprogenitor cell line (CPCL)A1 and CPCL3 cell migration in response to SDF-1 (200 ng/ml). $N \geq 3$; *, $p \leq .05$ compared with control groups with no added SDF-1. **(B):** Rat menisci containing a radial tear in the inner portion of the anterior horn was pretreated with SDF-1 recombinant protein (200 ng/ml) for 15 minutes followed by treatment with 1.0×10^5 fluorescently labeled CPCL3 cells. Images were acquired at the indicated time points. **(C):** Rat menisci containing a radial tear in the inner portion of the anterior horn was treated with 1.0×10^5 fluorescently labeled CPCL3 cells, in the presence of CXCR4 inhibitor AMD3100 (20 μ g/ml). Dotted lines help signify union and nonunion of the tissue periphery. Yellow arrows indicates partially filled tear channel. Blue arrow indicates completely filled tear channel.

differ (Fig. 5E). However, human COL10A1 mRNA levels were significantly elevated (>55-fold) in BM-MSCs, compared with CPCL3. These findings demonstrate that in comparison to BM-MSCs, human cartilage derived chondroprogenitors maintain significantly lower expression of type X collagen (a marker of cellular hypertrophy and prelude to endochondral ossification) during meniscus tissue repair. Additionally, basal type X collagen protein levels were measured between CPCL3 and BM-MSCs (Fig. 5F). Results indicated that BM-MSCs produce consistently higher levels of type X collagen protein, relative to CPCL3, thereby validating our findings at the protein level and further suggesting that C-PCs resist cellular hypertrophy and terminal differentiation.

Chondroprogenitor Cell Migration Via SDF-1/CXCR4 Axis Is Required to Successfully Fill Meniscus Tissue Tears

In order to understand the mechanism underlying the ability of C-PCs to efficiently migrate into and fill a meniscus tear, we investigated the involvement of stromal derived factor-1 (SDF-1) pathway in C-PC migration. SDF-1 is a chemokine secreted by damaged tissues that binds the CXCR4 receptor on target cells and mediates their migration to the site of injury [17, 18]. As such,

SDF-1 expression has been reported previously to be elevated in damaged meniscal tissues [19]. Inhibition of SDF-1 receptor CXCR4 has been reported to impede the homing of meniscus derived MSCs to regions of injury [19]. We first tested whether C-PCs, like BM-MSCs, are capable of migration in response to SDF-1 using a transwell assay. Both tested clonal C-PC lines CPCLA1 and CPCL3 migrated toward SDF-1 and exhibited approximately 60% increase in the number of migrated cells in the SDF-1 (200 ng/ml) containing bottom well (Fig. 6A). The proportion of migrating cells was comparable to that observed in the BM-MSC control group, which exhibited a 40% increase in migration toward the SDF-1 containing bottom well.

To better understand the role of SDF-1/CXCR4 activity in meniscus tissue repair, a radial tear was created in the ww zone of rat menisci. These menisci were either pretreated in explant culture with recombinant human SDF-1 protein, or treated with SDF-1/CXCR4 pathway inhibitor AMD3100. Each meniscus was then treated with 1.0×10^5 fluorescently labeled CPCL3 and the tears were imaged at multiple time points (Fig. 6B, 6C). It was demonstrated that pretreatment with recombinant SDF-1 protein led to better cell deposition onto the meniscus and along the banks of the tear channel in a linear orientation, as indicated by fluorescence imaging. This cell deposition ultimately resulted in complete filling of the

tear channel within 17 days following treatment with CPCL3 (Fig. 6B). On the other hand, AMD3100 treatment interfered with cellular deposition as less fluorescent signal was observed on the meniscus and along the meniscal tear channel (Fig. 6C). Ultimately, AMD3100 treatment prevented complete filling of the meniscus as the mouth of the radial tear remained visibly opened even after 20 days following treatment with CPCL3 (Fig. 6C). Additionally, AMD3100 treated samples exhibited unorganized CPCL3 aggregations that did not localize to the region of damage. These menisci showed evidence of impaired tear channel bridging. Taken together, these results indicate that intact SDF-1 chemokine pathway signaling is necessary to facilitate complete filling of meniscal tissue tears by C-PCs.

DISCUSSION

Articular C-PCs are sparse proliferative progenitors with multilineage differentiation potential [11]. These cells have been reported to have the ability to migrate to areas of cartilage distress/injury [20]. Given their specific tissue microenvironment, it has been previously proposed that these progenitors are primed for cartilaginous tissue repair and regeneration [21]. Although this is the inferred biological niche of C-PCs, the use of C-PCs in articular cartilage tissue repair needs to be further explored. No prior study has investigated the reparative capacity of C-PCs in the meniscus, which also consists of cartilaginous and fibrous tissue. Indeed, the most investigated cell-based meniscus repair strategies involve the use of stromal cells from the bone marrow to aid in the natural meniscal healing response [22]. BM-MSCs are capable of homing in and migrating to areas of injury and promoting tissue repair [23]. However, a reported limitation of utilizing BM-MSCs for cartilaginous tissue regeneration and repair is their propensity for hypertrophy during the chondrogenesis program [24–28]. The use of BM-MSCs alone for cell-based meniscus repair has been reported to have similar limitation [26]. Although it has been reported that coculturing meniscus derived progenitor cells with BM-MSCs in a specific ratios can reduce the expression of hypertrophy markers [26], this solution requires extraction of cells from the meniscus itself, which may be considered counterproductive. The use of alternative cell sources that are inherently less susceptible to hypertrophy and ossification may offer a simpler strategy.

In this study, we examined the heterogeneity of healthy human C-PCs by characterizing mixed primary C-PCs as well as different C-PC lines generated from individual cells representing pure clonal populations. We demonstrated that the generated cell lines do not significantly deviate from primary cells as they maintained a similar cell surface marker profile, mRNA expression profile, and retained the plasticity to differentiate along multiple cell lineages. We also demonstrated that human C-PCs can be distinguished from mature human chondrocytes based on their prominent expression of established MSC surface markers CD90 and CD166. Molecular characterization of C-PCs also confirmed that they express higher levels of the FN receptor ITGA5 and type I collagen as well as lower expression of chondrocyte markers SOX9 and aggrecan. Flow cytometry analysis confirmed that the collected primary healthy human C-PC was not contaminated with any cells of endothelial origin during isolation since CD106 expression was not observed. Although the cell surface marker profiles of primary healthy

human C-PC and primary healthy human BM-MSCs were similar (i.e., CD90+, CD166+, and CD106–), C-PCs were largely positive for CD54, which has been previously shown to be expressed by mature human chondrocytes [14, 29, 30].

Our findings demonstrated that the clonal cell lines we generated in order to further study C-PCs in healthy human cartilage exhibited similar cellular and molecular properties as primary heterogeneous (mixed population) C-PCs. Basal mRNA quantification and analysis revealed for the first time that unlike progenitors found in OA patient cartilage [14], every clonal C-PC line that came from healthy human cartilage exhibit significantly lower expression of type X collagen in comparison to BM-MSCs, which are currently the most commonly used MSCs in animal models of cell-based cartilage and meniscus repair [6]. This finding, in combination with our finding that C-PC lines exhibit higher expression of type I collagen than mature chondrocytes, became our primary motivation for testing the efficacy of C-PCs in meniscus tissue repair. Type I collagen is the primary building block of the meniscal extracellular matrix network and accounts for approximately 90% of its dry weight [31].

When we tested the reparative capacity of C-PCs, our results demonstrated that they can initiate reintegration of a meniscus tissue tear in explant culture. Clonal C-PC line CPCL3 and BM-MSCs filled the tear channel with varying degrees of efficiency, with CPCL3 achieving the fastest and most complete filling (within 20 days after seeding). Our study additionally revealed for the first time that C-PCs have a paracrine effect that improves the rate of meniscal fibrochondrocyte proliferation that is comparable (if not better) than the effects of BM-MSCs. Secretion of bioactive factors by C-PCs may play a critical role in mobilizing local cells to help mediate tissue repair. Also much improved in C-PC treated menisci was the significantly lower expression of hypertrophic marker collagen X mRNA level, in comparison to BM-MSC treated menisci. These findings supported our central hypothesis that C-PCs from healthy human cartilage resist cellular hypertrophy.

Both healthy and osteoarthritic cartilage contains progenitor/stem cell populations [11, 32]. It has been previously reported that osteoarthritic cartilage stem/progenitor cells (OASCs) are a population of CD166+ cells that exceedingly express hypertrophic marker collagen X, with respect to BM-MSCs [14]. OASCs also express diminished collagen I, in comparison to mature chondrocytes [14]. Although further comparison between healthy human C-PCs and OASCs is underway, these aforementioned features of OASCs are already in sharp contrast to healthy articular cartilage derived C-PCs. As such, it can be argued that C-PCs are suitable for use in fibrocartilage repair whereas OASCs are not.

A limitation of the present study is the use of stable cell lines because cell lines may deviate from the primary cells that were used to generate them. However, this limitation is not unique to our study as it applies to all studies using cell lines to arrive at a conclusion about the primary cells with which they were generated. We were aware of this limitation and confirmed early in the study that the cell surface profiles of primary C-PCs and stable C-PC cell lines were similar and that no obvious molecular deviations were introduced. By the same token, a notable innovation of the study is that it is the first (to the best of our knowledge) to demonstrate that a progenitor/stem cell line can be used to promote reintegration of meniscal tissue. Since the use of stabilized/immortalized cells

for clinical use is well outside current regulatory standards, it is imperative to develop means of isolating and expanding primary C-PCs moving forward.

From a translational perspective, a barrier to the use of C-PCs for tissue repair/regeneration is their low natural abundance. C-PCs consist of less than 1% of cells found in healthy articular cartilage [33,34]. Similarly, BM-MSCs also consist of <1% of all stromal cells in the bone marrow [35]. However, since BM-MSCs can be obtained simply from marrow aspirates, these cells are considered easier to obtain than C-PCs that require extraction from cartilage tissue itself. On the other hand, it can be argued that both stem/progenitor cell types need to be expanded in vitro to generate sufficient cell numbers for cell-based tissue repair applications after isolation. Hence, the true challenge is finding a viable cell source for C-PCs. Using a strategy that is like ACLI to isolate C-PCs from nonweight bearing regions of articular cartilage may be a potential avenue to obtain cells for expansion and use in cell-based meniscus repair.

Explant culture systems are inherently devoid of blood circulation. This suggests that initiation of the observed meniscal tissue healing/repair is possible without first forming a blood clot, provided that an influx of stem cells is readily available near the damage site. The present proof of concept study demonstrates the reparative capabilities of C-PC lines on meniscal fibrocartilage. We report for the first time that C-PCs (like BM-MSCs) are capable of migrating to areas of injury where the chemokine SDF-1 is produced [19]. Ablation of SDF-1/CXCR4 signaling by pathway inhibitor AMD3100 prevented complete meniscus integration by C-PCs. This confirmed our hypothesis that SDF-1/CXCR4 axis plays an important role in promoting meniscal tear filling and tissue integration by C-PCs in our ex vivo model. Overall, the present study provides rationale for the future investigation of the use of C-PCs in articular soft tissue repair/regeneration applications.

CONCLUSION

This study demonstrates that clonal progenitor cells isolated from human articular cartilage have the ability to bridge and

reintegrate torn meniscal fibrocartilage. These cells can migrate to the area of injury and mediate tissue repair in a manner that relies on SDF-1/CXCR4 chemokine axis activity. The study additionally shows that cartilage-derived progenitors are resistant to mRNA and protein expression of hypertrophic differentiation marker type X collagen, relative to bone-marrow derived MSCs, which is currently the most used cell source for emerging preclinical cell-based connective tissue repair strategies. Overall, this study introduces a novel cellular tool to improve fibrocartilage repair in meniscus tissue.

ACKNOWLEDGMENTS

This article is dedicated to the loving memory of a wonderful mentor and visionary in the field of orthopedic research, Dr. Michael Gary Ehrlich (1939–2018). This study was supported by Institutional Development Award Number NIH U54GM115677 from the National Institute of General Medical Sciences (NIGMS), which funds Advance Clinical and Translational Research (Advance-CTR).

AUTHOR CONTRIBUTIONS

C.T.J.: conception and design, collection and assembly of data, data analysis and interpretation, manuscript writing, final approval of manuscript; J.T.K.: collection and assembly of data, data analysis and interpretation, final approval of manuscript; J.N.: collection and assembly of data, final approval of manuscript; S.D.: collection of data, manuscript writing, final approval of manuscript; P.F., J.R.F.: collection of data, final approval of manuscript; N.L., R.T.: provision of study material or patients, final approval of manuscript; M.G.E., B.D.O.: data analysis and interpretation, final approval of manuscript.

DISCLOSURE OF POTENTIAL CONFLICTS OF INTEREST

B.D.O. declared consultant/advisory role with Consultant Mitek, Conmed/MTF, Vericel. The other authors indicated no potential conflicts of interest.

REFERENCES

- Majewski M, Susanne H, Klaus S. Epidemiology of athletic knee injuries: a 10-year study. *Knee* 2006;13:184–188.
- Bray RC, Smith JA, Eng MK et al. Vascular response of the meniscus to injury: effects of immobilization. *J Orthop Res* 2001;19:384–390.
- Terry Canale S, Beaty J. *Campbell's Operative Orthopaedics*. 12th ed. St Louis, MO: Elsevier, 2012.
- Papalia R, Del Buono A, Osti L et al. Meniscectomy as a risk factor for knee osteoarthritis: a systematic review. *Br Med Bull* 2011;99:89–106.
- Bilgen B, Jayasuriya CT, Owens BD. Current concepts in meniscus tissue engineering and repair. *Adv Healthc Mater* 2018;7:e1701407.
- Korpershoek JV, de Windt TS, Hagmeijer MH et al. Cell-based meniscus repair and regeneration: at the brink of clinical translation? A systematic review of preclinical studies. *Orthop J Sports Med* 2017;5:2325967117690131.
- Makris EA, Hadidi P, Athanasiou KA. The knee meniscus: structure-function, pathophysiology, current repair techniques, and prospects for regeneration. *Biomaterials* 2011;32:7411–7431.
- Caplan AI, Dennis JE. Mesenchymal stem cells as trophic mediators. *J Cell Biochem* 2006;98:1076–1084.
- Pabbruwe MB, Kafienah W, Tarlton JF et al. Repair of meniscal cartilage white zone tears using a stem cell/collagen-scaffold implant. *Biomaterials* 2010;31:2583–2591.
- Zellner J, Hierl K, Mueller M et al. Stem cell-based tissue-engineering for treatment of meniscal tears in the avascular zone. *J Biomed Mater Res B Appl Biomater* 2013;101:1133–1142.
- Dowthwaite GP, Bishop JC, Redman SN et al. The surface of articular cartilage contains a progenitor cell population. *J Cell Sci* 2004;117:889–897.
- Ossendorf C, Steinwachs MR, Kreuz PC et al. Autologous chondrocyte implantation (ACI) for the treatment of large and complex cartilage lesions of the knee. *Sports Med Arthrosc Rehabil Ther Technol* 2011;3:11.
- Williams R, Khan IM, Richardson K et al. Identification and clonal characterisation of a progenitor cell sub-population in normal human articular cartilage. *PLoS ONE* 2010;5:e13246.
- Jayasuriya CT, Hu N, Li J et al. Molecular characterization of mesenchymal stem cells in human osteoarthritis cartilage reveals

contribution to the OA phenotype. *Sci Rep* 2018;8:7044.

15 Li J, Hansen KC, Zhang Y et al. Rejuvenation of chondrogenic potential in a young stem cell microenvironment. *Biomaterials* 2014;35:642–653.

16 Alsalameh S, Amin R, Gemba T et al. Identification of mesenchymal progenitor cells in normal and osteoarthritic human articular cartilage. *Arthritis Rheum* 2004;50:1522–1532.

17 Kucia M, Jankowski K, Reza R et al. CXCR4/SDF-1 signalling, locomotion, chemotaxis and adhesion. *J Mol Histol* 2004;35:233–245.

18 Suratt BT, Petty JM, Young SK et al. Role of the CXCR4/SDF-1 chemokine axis in circulating neutrophil homeostasis. *Blood* 2004;104:565–571.

19 Shen W, Chen J, Zhu T et al. Intra-articular injection of human meniscus stem/progenitor cells promotes meniscus regeneration and ameliorates osteoarthritis through stromal cell-derived factor-1/CXCR4-mediated homing. *STEM CELLS TRANSLATIONAL MEDICINE* 2014;3:387–394.

20 Seol D, McCabe DJ, Choe H et al. Chondrogenic progenitor cells respond to cartilage injury. *Arthritis Rheum* 2012;64:3626–3637.

21 Koelling S, Miosge N. Stem cell therapy for cartilage regeneration in osteoarthritis. *Expert Opin Biol Ther* 2009;9:1399–1405.

22 Yu H, Adesida AB, Jomha NM. Meniscus repair using mesenchymal stem cells—a

comprehensive review. *Stem Cell Res Ther* 2015;6:86.

23 De Becker A, Riet IV. Homing and migration of mesenchymal stromal cells: how to improve the efficacy of cell therapy? *World J Stem Cells* 2016;8:73–87.

24 Cui X, Hasegawa A, Lotz M et al. Structured three-dimensional co-culture of mesenchymal stem cells with meniscus cells promotes meniscal phenotype without hypertrophy. *Biotechnol Bioeng* 2012;109:2369–2380.

25 Matthies NF, Mulet-Sierra A, Jomha NM et al. Matrix formation is enhanced in co-cultures of human meniscus cells with bone marrow stromal cells. *J Tissue Eng Regen Med* 2013;7:965–973.

26 Saliken DJ, Mulet-Sierra A, Jomha NM et al. Decreased hypertrophic differentiation accompanies enhanced matrix formation in co-cultures of outer meniscus cells with bone marrow mesenchymal stromal cells. *Arthritis Res Ther* 2012;14:R153.

27 Sekiya I, Vuoristo JT, Larson BL et al. In vitro cartilage formation by human adult stem cells from bone marrow stroma defines the sequence of cellular and molecular events during chondrogenesis. *Proc Natl Acad Sci U S A* 2002;99:4397–4402.

28 Yoo JU, Barthel TS, Nishimura K et al. The chondrogenic potential of human bone-marrow-derived mesenchymal progenitor cells. *J Bone Jt Surg Am* 1998;80:1745–1757.

29 Lee HJ, Choi BH, Min BH et al. Changes in surface markers of human mesenchymal stem cells during the chondrogenic differentiation and dedifferentiation processes in vitro. *Arthritis Rheum* 2009;60:2325–2332.

30 Kienzle G, von Kempis J. Vascular cell adhesion molecule 1 (CD106) on primary human articular chondrocytes: functional regulation of expression by cytokines and comparison with intercellular adhesion molecule 1 (CD54) and very late activation antigen 2. *Arthritis Rheum* 1998;41:1296–1305.

31 Fox AJ, Bedi A, Rodeo SA. The basic science of human knee menisci: structure, composition, and function. *Sports Health* 2012;4:340–351.

32 Koelling S, Kruegel J, Irmer M et al. Migratory chondrogenic progenitor cells from repair tissue during the later stages of human osteoarthritis. *Cell Stem Cell* 2009;4:324–335.

33 Hattori S, Oxford C, Reddi AH. Identification of superficial zone articular chondrocyte stem/progenitor cells. *Biochem Biophys Res Commun* 2007;358:99–103.

34 Jayasuriya CT, Chen Q. Potential benefits and limitations of utilizing chondroprogenitors in cell-based cartilage therapy. *Connect Tissue Res* 2015;56:265–271.

35 Pittenger MF, Mackay AM, Beck SC et al. Multilineage potential of adult human mesenchymal stem cells. *Science* 1999;284:143–147.



See www.StemCells.com for supporting information available online.